DOI: 10.3901/CJME.2011.06.***, available online at www.cjmenet.com; www.cjmenet.com.cn

# Regenerative Braking Strategy for Motor Hoist by Ultracapacitor

BIAN Yongming, ZHU Lijing*, LAN Hao, LI Anhu, and XU Xinming

*School of Mechanical Engineering, Tongji University, Shanghai 201804, China*

Received November 11, 2010; revised June 3, 2011; accepted June 28, 2011; published electronically July 12, 2011

**Abstract:** Rising concern in environmental issues on global scale has made energy saving in powered equipment a very important subject. In order to improve the energy efficiency and driving range of a motor hoist, a regenerative braking system is designed and discussed. The system takes a unique ultracapacitor-only approach to energy storage system. The bi-directional bride DC/DC converter which regulates current flow to and from the ultracapacitor operates in two modes: boost and buck, depending on the direction of the flow. In order to provide constant input and output current at the ultracapacitor, this system uses a double proportional-integral (PI) control strategy in regulating the duty cycle of PWM to the DC/DC converter. The permanent magnet synchronous motor (PWSM) drive system is also studied. The space vector pulse width modulation (SVPWM) technique, along with a two-closed-loop vector control model, is adopted after detailed analysis of PMSM characteristics. The overall model and control strategy for this regenerative braking system is ultimately built and simulated under the MATLAB and Simulink environment. A test platform is built to obtain experimental results. Analysis of the results reveals that more than half of the gravitational potential energy can be recovered by this system. Simulation and experimentation results testify the validity of the double PI control strategy for interface circuit of ultracapacitor and SVPWM strtegy for PMSM.

**Key words:** ultracapacitor, regenerative braking stratege, DC/DC converter, permanent magnet synchronous motor, space vector pulse width modulation

## 1 Introduction

As issues of climate change and energy crisis are gathering more and more attention worldwide, industrialized nations have increased effort to reduce fossil fuel usage. One of the most significant steps in this effort is to change the power source of automobiles and construction vehicles from heat engines to variable speed motors. Not only is the variable speed motor drive system generally more efficient, it can also utilize electric power generated from renewable sources such as wind and solar. Variable speed motor drive does have technical problem of its own, however: quick acceleration and deceleration in the drive, as the application often requires, put the power source under transient but large voltage fluctuations. The cheap and easy solution is to add a braking resistor to the inverter DC link, but it leads to considerable waste. A more common and sophisticated solution is to incorporate an energy storage system (ESS) into the system to absorb the energy while braking and regenerate it when needed. Energy storage system[1–8] has seen applications in electric vehicles (EV), hybrid electric vehicles (HEV) and plug-in hybrid electric vehicles.

Traditionally electrical ESS embraces a broad range of technologies and comes in a variety of forms, such as electrochemical systems (e.g. batteries, flow cells), kinetic energy storage (e.g. flywheel) and potential energy storage (e.g. pumped hydroelectric, compressed air) [9].

The development of ultracapacitor[10–12] has provided an attractive alternative for the next-generation pure-electric vehicles. Recent research results have proposed many methods to use ultracapacitors in the regenerative braking system. WEI and WANG[13] presented the performance analysis and comparison of three kinds of typical configurations to clarify the advantages and disadvantages of different topologies. XU and XIE[14] devoted their research into the voltage-equalization method for series ultracapacitors in EV/HEV ESS. A new battery/ultracapacitor hybrid energy storage system (HESS), using a much smaller DC/DC converter to maintain the voltage of the ultracapacitor, was proposed by CAO and EMADI[15] for EV, HEV and plug-in HEV. YAN and PATTERSON[16] presented a novel power management scheme to achieve high performance and cost reduction in an electric vehicle

* Corresponding author. E-mail: zhulijing126@126.com
This project is supported by National Key Technology Research and Development Program of China (Grant No. 2007BAF10B00)

for short profile fleet application. Zinc-bromine batteries are employed to provide the continuous power for normal driving while ultracapacitors are employed to provide for peak power demand during acceleration and to store regenerative braking energy during deceleration. The EV motor operates in constant torque mode at a speed below the base speed and in constant power mode at a speed over the base speed for high efficiency and low cost. AHMED and CHEMIELEWSKI[17] have built a model aimed at mimicking the load expected in a fuel cell vehicle, including a DC motor, DC/DC converters and a rechargeable battery for peak-shaving and regenerative braking. This model also includes the kinematics of the vehicle, and thus can be connected to standardized drive cycle scenarios. LU and CORZINE[18] introduced a new set of methods to directly integrate ultracapacitor banks into cascaded multilevel inverters that are used for large vehicle propulsion. The idea is to replace the regular DC link capacitors with ultracapacitors in order to combine the energy storage unit and motor drive. These researches have all demonstrated the using ultracapacitor as a viable supplementary storage device to batteries in hybrid vehicles to extend the battery life. Ultracapacitor has been considered as an auxiliary power source which can assist the fuel cell during startup and fast power transients of fuel-cell powered vehicles.

Currently there has been no documented research on ultracapacitor-based ESS applied to hoisting equipment. In this research, an ultracapacitor-only energy storage system for motor hoist will be adopted, which differs from the traditional vehicle regenerative braking system's ultracapacitor/battery hybrid approach. The ultracapacitor-only energy storage system can simplify the circuit structure and expand the control bus greatly.

First, the control schemes for permanent magnet synchronous motor (PMSM) and DC/DC converter will be separately discussed. Then a DSP-based control system is developed based on the control strategy and digital signal processing technique. The overall system structure and control strategy are subsequently studied. An implementation scheme of the regenerative braking system has been developed and built for this experiment. At last, the simulation results and experimental results are compared and the efficiency of the entire energy recovery system is analyzed.

## 2 Ultracapacitor Energy Storage System

### 2.1 Control strategy of DC/DC converter

Ultracapacitor with the advantages of high charge rate, high efficiency, high power density, long cycle life, no maintenance[19], is preferred as the energy storage for motor hoist. The ultracapacitor as energy storage unit is integrated into inverter DC link through a DC/DC converter. The DC/DC converter can work as a boost or buck converter depending on input-output conditions.

Fig. 1 shows PSIM simulation model of the boost operation of the DC/DC converter. The boost operation is used for driving PMSM and discharging the ultracapacitor. The IGBT2 is switched on and off at a controlled duty cycle, to transfer the required amount of energy from the ultracapacitor to the DC link. When IGBT2 is switched ON, energy is taken from the ultracapacitor and stored in the inductor L1. When IGBT2 is switched OFF, the energy stored in L1 is transferred into DC link through D1. When discharges ultracapacitors, the converter is used as a stiff voltage source to electric motor controller. The boost converter adjusts voltage automatically and then get a steady output voltage. To ensure that the ultracapacitor works in a safe, reliable and high efficient condition, double PI closed-loop is adopted.

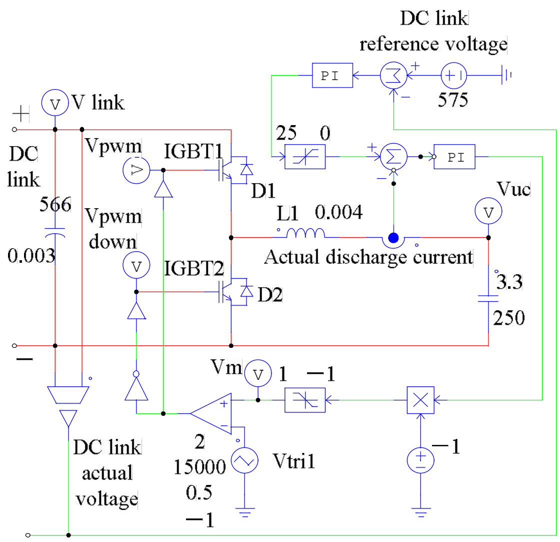


Fig. 1. Control principle of boost converter

As shown in Fig. 2, the DC/DC converter works as a buck converter, which used for charging the ultracapacitor during regenerative braking. During the buck operation, the converter transfers energy from the DC link to the ultracapacitor. That operation is accomplished by a controlled operation on IGBT1. When IGBT1 is switched on, the energy goes from the link bus to the ultracapacitor, and inductor L1 stores part of this energy. When IGBT1 is switched OFF, the remaining energy stored in inductor L1 is transferred into the ultracapacitor through D2. Double PI closed-loop control strategy is used for regulating the duty cycle of PWM of the IGBTs. The DC/DC converter current becomes pulsating current as IGBTs periodically turning on and off, however, the output current keeps continuous and smooth, owing to the effect of inductance coil, freewheeling diode and filter capacitor. If the load is resistive, the output DC voltage also keeps continuous and smooth. The DC/DC converter maintains constant voltage of the inverter DC link, whereas the ultracapacitor voltage has wide variation ranges.

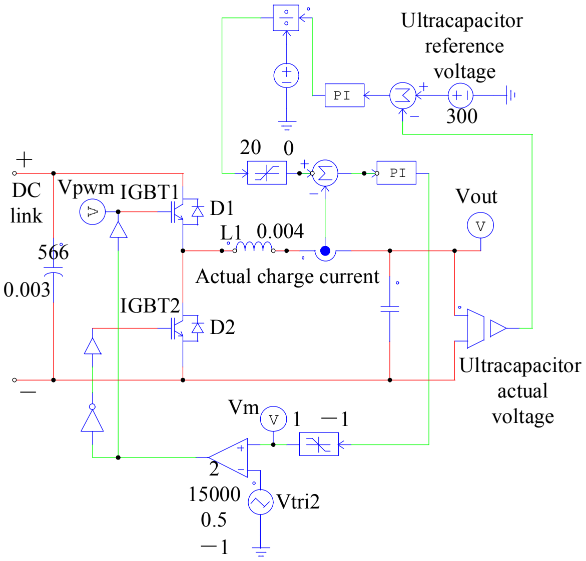


Fig. 2. Control principle of buck converter

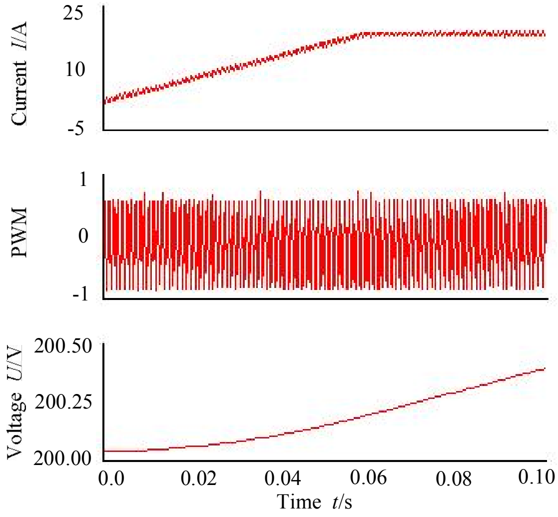


(b) Buck simulation results

Fig. 3. Simulation results

## 2.2 Simulation and experiment results of the DC/DC converter

To evaluate the effectiveness and availability of the control principle of the regenerative braking energy system, the system PSIM simulation models of DC/DC converter are established under buck and boost operation condition respectivly. The boost and buck converter simulation results are shown in Fig. 3(a) and Fig. 3(b) respectively. The results show that the voltage of ultracapacitor step up or down 8 V per second at current 25 A.

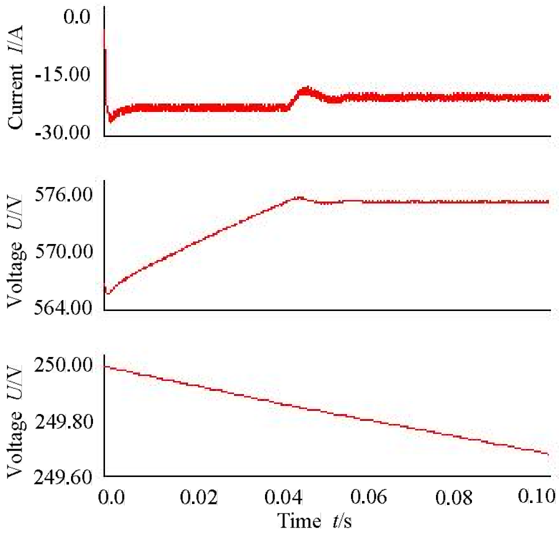


(a) Boost simulation results

The motor no-load experiment is carried out during a cycle-life of the ultracapacitor. Fig. 4(a)–Fig. 4(b) shows the experiment results, including the velcity of motor, the ultracapacitor current, DC link voltage and ultracapacitor voltage. The data shows that in a cycle, the discharging time is about 170 s and the charging time is about 45s. The DC link voltage is about 570 V while ultracapacitor is discharged, and is 540 V when charged. The maximum voltage of the ultracapacitor is 300 V and the minimum voltage is 200 V. Compared with Fig. 3(a), the discharging current of the ultracapacitor is more smooth, because the motor is resistive.

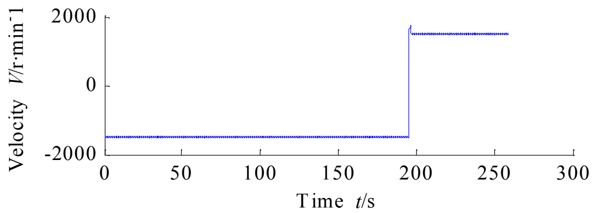


(a) Velcity of PMSM

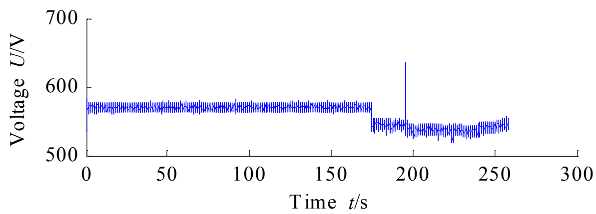


(b) Voltage of DC

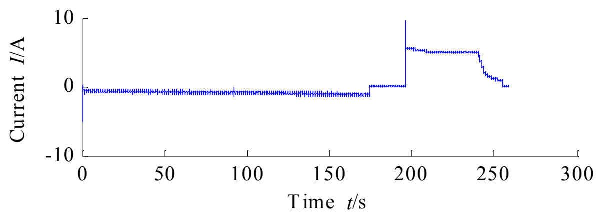


(c) Current of ultracapacitor

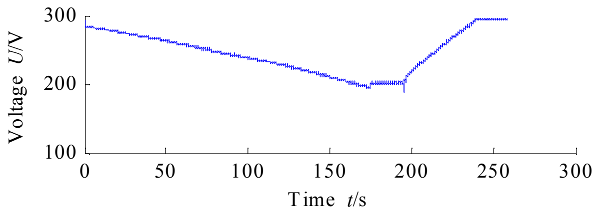


(d) Voltage of ultracapacitor

Fig. 4. Motor no-load experimental results

## 3 Vector-Control for PMSM

### 3.1 Mathematical modeling of PMSM

Permanent magnet synchronous motor (PMSM) has been widely used due to its high power density, efficiency, high large torque-to-inertia ratio and reliable operation. The PMSM operates in either generator or motor mode. The operation mode is dictated by the rotating rate deviation of the magnetic field generated by the stator and rotor (positive for motor mode, negative for generator mode).

The PMSM discussed in this paper has these assumptions: the core saturation and machine winding leakage inductance are ignored; the magnetic potential in the air gap is assumed to be in sine distribution; the higher harmonic wave in magnetic field is negligible. According to the coordinate transformation principle, the mathematic model of PMSM can be expressed by such equations in the rotating reference frame ( *d*-*q* reference frame):

$$\frac{\mathrm{d}}{\mathrm{d}t}i_d = \frac{1}{L_d}v_d - \frac{R}{L_d}i_d + \frac{L_q}{L_d}p\omega_r i_q , \tag{1}$$

$$\frac{\mathrm{d}}{\mathrm{d}t}i_q = \frac{1}{L_q}v_q - \frac{R}{L_q}i_q + \frac{L_d}{L_q}p\omega_r i_d - \frac{\lambda p\omega_r}{L_q} , \tag{2}$$

$$T_e = \frac{3}{2}p[\lambda i_q + (L_d - L_q)i_d i_q] , \tag{3}$$

where $L_q$ , $L_d$ —*q* and *d* inductances, respectively;

$R$ —Resistance of the stator windings;

$i_q, i_d, V_q, V_d$—q and d axis currents and voltages, respectively;

$\omega_r$ —Angular velocity of the rotor;

$\lambda$ — Amplitude of the flux induced by the permanent magnets of the rotor in the stator phases;

$p$ —Number of pole pairs;

$T_e$—Electromagnetic torque.

The mechanical dynamic equation is given by

$$Jpw = -fw + T_e - T_L , \tag{4}$$

where $T_L$ —Load torque;

$f$ —Friction coefficient of the motor;

$J$ —Moment of inertia of the motor.

### 3.2 Principle of SVPWM

The Space Vector Pulse Width Modulation (SVPWM) technique is widely used in inverter[20–21]. The stator flux space vector rotates in a constant velocity with invariable amplitude when it is supplied by 3-phase sinusoidal voltage. Meanwhile, the movement of flux vector forms a circular space rotating field. The same is true with voltage vector. When flux vector rotates a period in space, the voltage vector also rotates a period following the tangent line of the flux circle. Therefore, its trajectory coincides with the flux circle. The SVPWM is a technology that uses eight space voltage vectors to generate flux circle approaching stator flux circle of the motor.

The space vector pulse width modulation technique is used to excite the motor with the calculated stator voltage space vector via a voltage source inverter. In this paper, two closed-loop vector control model for Space Vector Pulse Width Modulation is adopted. Fig. 5 presents the block diagram of the proposed control scheme.

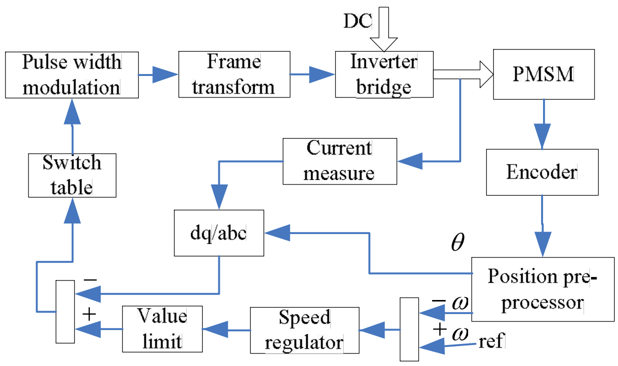


Fig. 5. Block diagrame of the proposed control system

## 4 System Structure

### 4.1 Energy control strategy

Motor hoist is frequently used in construction. As shown in Fig. 6, the motor hoist with regenerative energy system is mainly composed of ultracapacitor, DC/DC converter, encoder, three-phase inverter, PMSM, microprocessor DSP, detection systems and hardware protection.

The encoder detects the PMSM speed and direction. The hall sensor detects voltage, current and temperature of the ultracapacitor and DC link. The microprocessor DSP not only adjusts the DC/DC converter between buck and boost operation, but also controls the motor speed and direction on the basis of sensors signals. Protection system will cut off the circuit automatically if the temperature or current is too high.

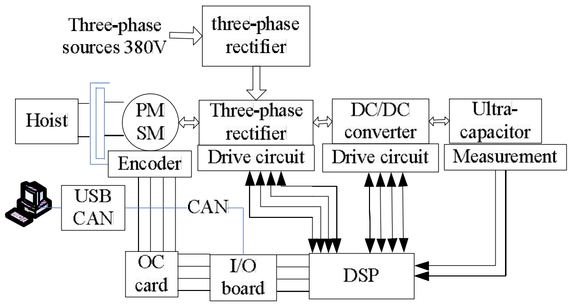


Fig. 6. Schematic diagrame of regenerative braking system for motor hoist main hardware circuit

Power management strategy is as follows: when the load drops, the motor works as a generator. During this process, if the ultracapacitor voltage is less than 300 V the DC/DC converter will work in buck operation and charge the ultracapacitor until the ultracapacitor voltage is up to 300 V. Then the ultracapacitor will be cut off and the electric resistance braking will be adopted. However, during the process of hoisting load, if the ultracapacitor voltage is higher than 200 V, the DC/DC converter will work in boost operation and discharge the ultracapacitor. But if the ultracapacitor voltage is less than 200 V, the motor will be fed by AC 380 V power to replace the ultracapacitor as energy sources. To realize a safe, reliable and efficient operation, the ultracapacitor is charged and discharged at various constant current under 20 A and its voltage is in the range of 200–300 V. The operating mode of the bi-directional DC/DC converter depends on the internal energy of ultracapacitor and the working station of PMSM.

### 4.2 Simulation of regenerative braking system

To evaluate feasibility of this regenerative braking system, simulations are performed based on MATLAB/Simulink, as shown in Fig. 7.

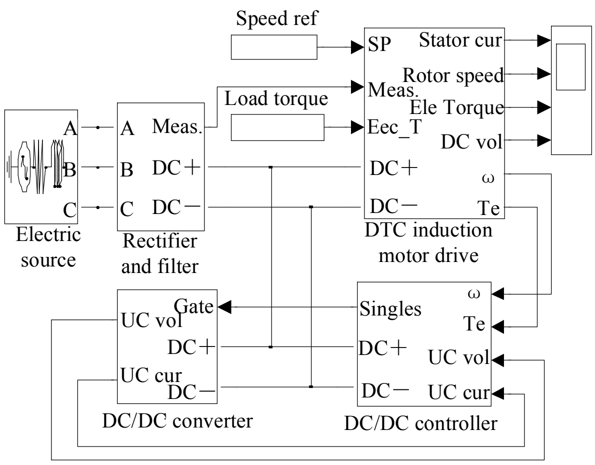


Fig. 7. Matlab model of regenerative braking system

The motor circuit uses a direct torque control (DTC) induction motor drive with space vector pulse width modulation during speed regulation. The induction motor is fed by a PWM voltage source inverter. The speed control loop uses a PI controller to produce the flux and torque references for the DTC block. The DTC block computes the motor torque and flux estimates and compares them to their respective reference. The torque and flux are then controlled by independent PI regulators that compute a reference voltage vector. The voltage source inverter is then controlled by the space vector modulation method in order to output the desired reference voltage.

The electrical system contains also a DC/DC converter. Here, the DC/DC converter is to adapt ultracapacitor to the DC link. The DC/DC converter can work as either boost or buck converter, depending on the ultracapacitor internal energy and the PMSM working state.

At time $t$ = 0 s, the motor speed is set at 1 500 r/min. Then a negative reference speed ramp of −1 500 r/min is applied to motor at $t$ = 20 s. Correspondingly, the load is hoisted up first and the ultracapacitor is discharged. Then the load is lowered down and the ultracapacitor is charged. The simulation results of the ultracapacitor signals (voltage and current), DC link signal (voltage) and the motor signals are shown in Fig. 8 and Fig. 9.

As Fig. 8(a)–Fig. 8(c) shown, when load goes up, the voltage of ultracapcitor drops down from 250 V to 200 V. Then the voltage keeps constant until the PMSM reverses. Subsequently, in process of the load going down, the ultracapacitor current is approximate to 10 A, voltage start to increase and reaches to 244 V at $t$ = 40 s. But the ultracapacitor will be cut off from the DC link, if the ultacapacitor voltage is below 200 V when hoisting load or above 300 V when lowering load.

As Fig. 8(d)–Fig. 8(f) shown, motor driving starts at almost full load. When velocity direction changes at $t$ = 20 s, the motor start to be driven by external load and operates as a generator. At this moment the motor electric torque immediately drops down to approximate to zero in order to maintain the regulated speed. When the speed reaches the set value of negative 1 500 r/min, the electric torque stabilizes at negative 11 N m.

Fig. 9 shows the experimental results under the same condition of Fig. 8 except for the ultracapacitor charge-discharge current at 5 A. First, the voltage of the ultracapcitor reduces from 250 V to 218 V, then it swells upto 248 V. Comparing Fig. 8 and Fig. 9, the following conclusions can be drawn, on the condition of same external load and at the same motor speed, higher the ultracapacitor charge-discharge current is, more the energy is regenerated.

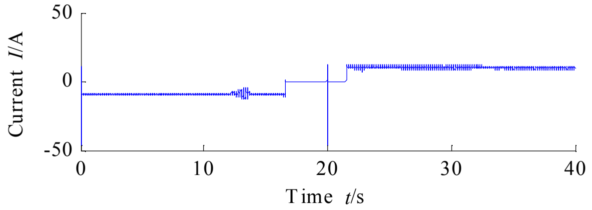


(a) Current of ultracapacitor

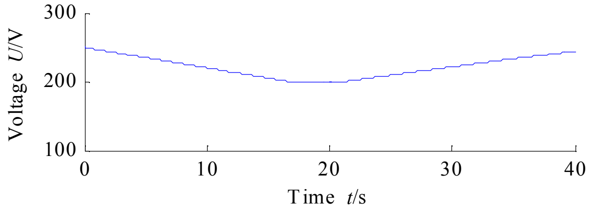


(b) Voltage of ultracapacitor

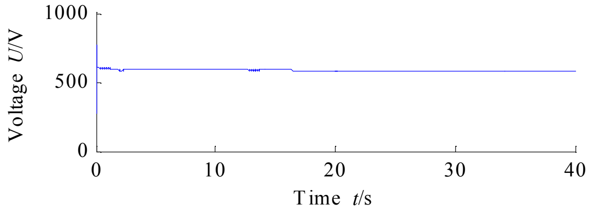


(c) Voltage of DC

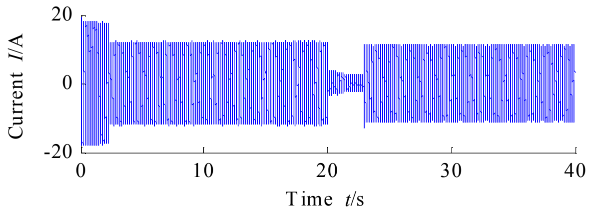


(d) Current of PMSM

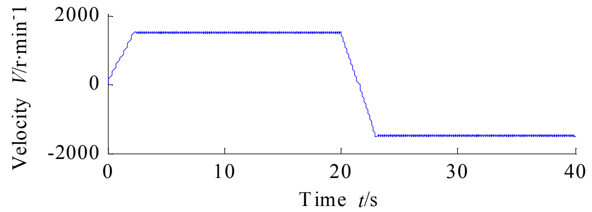


(e) Velcity of PMSM

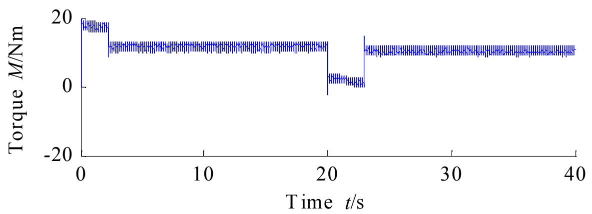


(f) Electromagnetic torque

Fig. 8. Simulation results at 10A

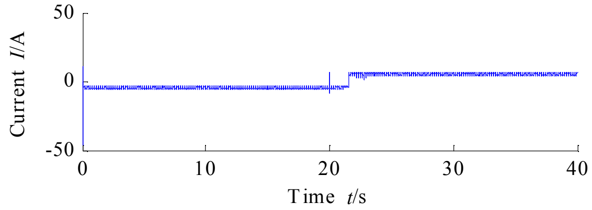


(a) Current of ultracapacitor

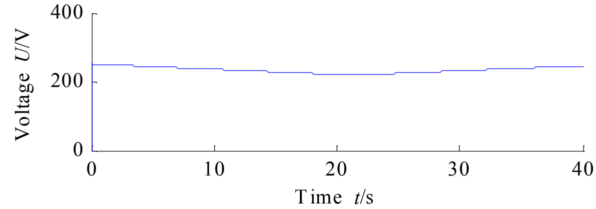


(b) Voltage of ultracapacitor

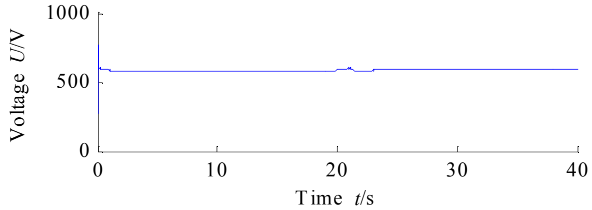


(c) Voltage of DC

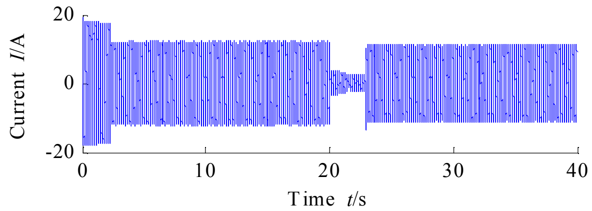


(d) Current of PMSM

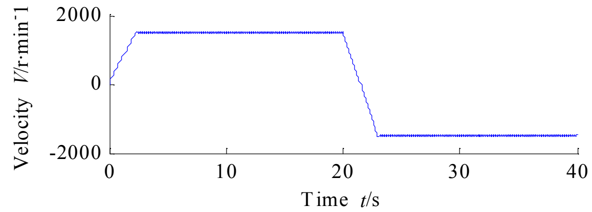


(e) Velcity of PMSM

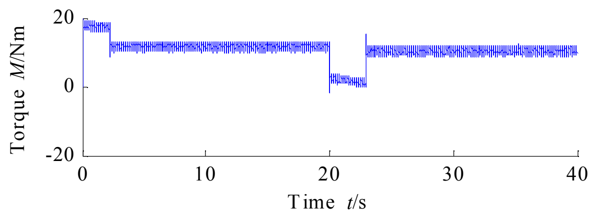


(f) Electromagnetic torque

Fig. 9. Simulation results at 5A

## 5 Force Feedback Experiments

Fig. 10 shows the overall views of experimental apparatus. The related parameters and specifications are shown in Table. One cycle of the driving pattern consists of starting from rest, acceleration, high-speed running, inverted running and stop.

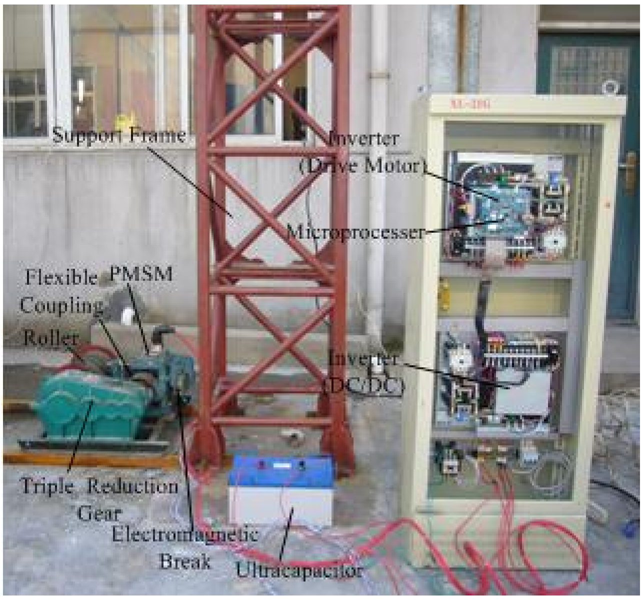


Fig. 10. Laboratory setup

**Table. Related parameters of the motor hoist**

| Parameter | | Value |
|---|---|---|
| Motor type | | PMSM |
| Motor power $J$/kW | | 7.5 |
| Ultracapacitor | Capacity $C$/F | 3.3 |
| | Working voltage $U$/V | 200–300 |
| | Connecting type | 120 in series |
| Inductance | Inductance $L$/mH | 4.0 |
| | Rated Current $I$/A | 25 |
| | Frequency $f$/kHz | 15 |
| Pull Force $F$/KN | | 10 |
| Total ratio $\eta$/% | | 60.57 |
| Lifting height $h$/m | | 5 |
| Load mass $m$/kg | | 700 |

Fig. 11 shows the experimental results, including the motor speed, DC link voltage, the instantaneous current and actual voltage of the ultracapacitor at 10A charge-discharge current. As the Fig. 11 shows, the motor runs at 1 500 r/min in the first 20 s, then it changes direction and the speed goes up to 1 500 r/min. The voltage of the inverter DC link is about 600 V when the ultracapacitor is charged, as well as it is 570 V when the ultracapacitor is discharged. As the load goes lower, the voltage of ultracapacitor rises from 200 V to 232 V and the charging current is about 10 A. As the load goes up, the ultracapacitor discharging current is propinquity to –10 A.

The electric potential energy equation of the ultracapacitor is as follows:

$$E_e = \frac{1}{2}C\left(U_{const}^2 - U_{int}^2\right). \tag{5}$$

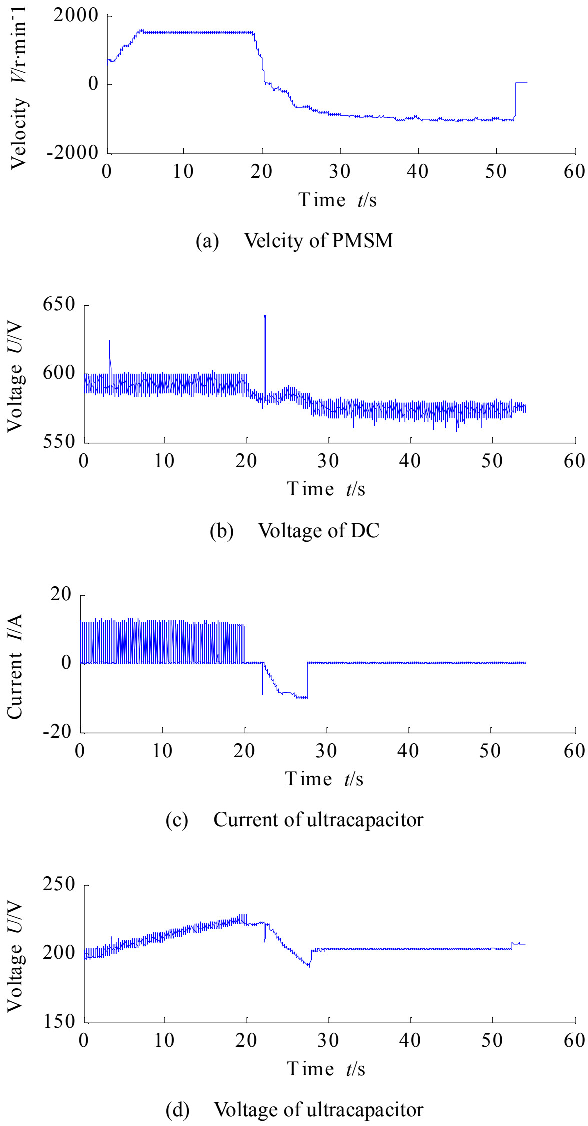


Fig. 11. Experimental results when ultracapacitor charge-discharge current is 10 A

The gravitational potential energy of the load is $E_G = mgh$ and the total mechanical efficiency is $\eta_m = 0.8$. According to the experimental results, energy conversion efficiency from the mechanical energy to electric potential energy is $\eta_e = 0.83$. The energy recovery rate is $\eta = 0.65$.

Fig. 12 shows the experimental results at 5 A charge-discharge current of the ultracapacitor. The energy conversion efficiency from the mechanical energy to electric potential energy is 0.72. The energy recovery rate is 0.58. Comparing Fig. 12 with Fig. 11, the recovery energy is more at 10 A than at 5 A.

Comparing the experimental results with the simulation results, the experimental value is lower than the simulation value, because the simulation is studied in an ideal state and ignores the energy losing during the energy conversion process.

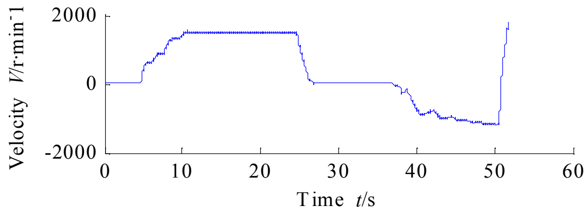


(a) Velcity of PMSM

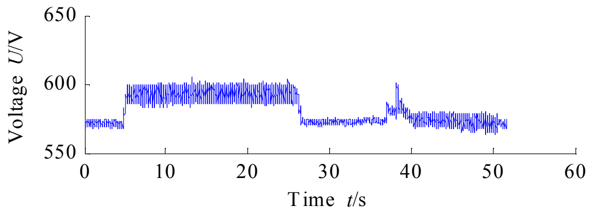


(b) Voltage of DC

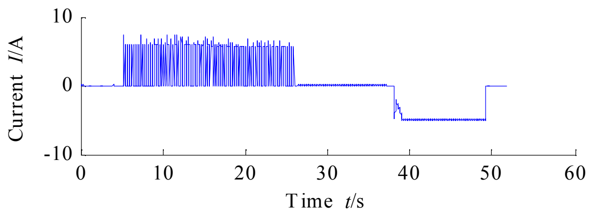


(c) Current of ultracapacitor

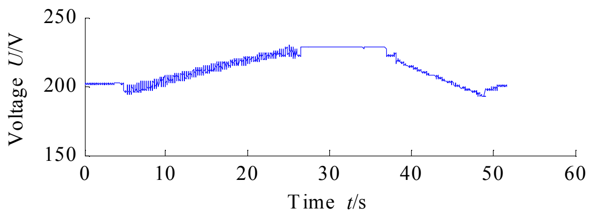


(d) Voltage of ultracapacitor

Fig. 12. Experimental results when ultracapacitor charge-discharge current is 5A

## 6 Conclusions

(1) Application of ultracapacitor energy storage system in motor hoist has been introduced from the system structure and control strategy perspective in detail. The control strategy ensures that the ultracapacitor and PMSM operate safely and efficiently. The control strategy is designed in detail and simulated.

(2) The loading experiment proved that the control strategy is stable and reliable. After this study, a theoretical basis has been established for the application of the ultracapacitor energy regeneration system to hoisting equipments and other construction machineries.

Further work on recovery system for large-scale synchronous hoisting equipment with ultracapacitor is underway.

## References

[1] YANG Ming-Ji, JHOU Hong-Lin. A Cost-Effective Method of Electric Braking With Energy Regeneration for Electric Vehicles[J]. *IEEE Transactions on Industrial Electronics*, June, 2009, 56(6): 2 203–2 212.

[2] ROTENBERG D, VAHIDI A V. Ultracapacitor assisited powertrains: modeling, control, sizing, and the impact on fuel economy[C]//*2008 American Control Conference,* Washington, USA, June 11–13, 2008: 981–987.

[3] AWERBUCH J J，SULLIVAN C R. Control of ultracapacitor-battery hybrid power source for vehicular applications[C]//*IEEE Energy 2030 Atlanta.* Georgia, USA, November 17–18, 2008.

[4] BANVAIT H, ANWAR S. A Rule-based energy management strategy for plug-in hybrid electric vehicle[C]//*2009 American control conference*. Hyatt Regency Riverfront, St. Louis, MO, USA, June 10–12, 2009: 3 938–3 943.

[5] SUN Hui, JIANG Jihai. Parameters matching and control method of hydraulin hybrid vehicle with secondary regulation technology[J]. *Chinese Journal of Mechanical Engineering,* 2009, 22(1): 57–63.

[6] MORENO J, ORTUZAR M E. Energy-management system for a hybrid electric vehicle, using ultracapacitors and neural networks[J]. *IEEE Transactions on Industrial Electronics,* 2006, 53(2): 614–623.

[7] MILLER J M, BOHN T. Why hybridization of energy storage is essential for future hybrid, plug-in and battery electric vehicles[J]. *IEEE,* 2009: 2 614–2 620.

[8] XIONG Weiwei, YIN Chengliang. Series-parallel hybrid vehicle control strategy design and optimization using rea-valued genetic algorithm[J]. *Chinese Journal of Mechanical Engineering,* 2009, 22(6): 862–868.

[9] BAKER J. New technology and possible advances in energy storage[J]. *Energy Policy,* 2008, 36: 4 368–4 373.

[10] BERTRAND J, SABATIER J. Fractional non-linear modelling of ultracapacitors[J]. *Commun Nonlinear Sci Numer Simulat,* 2010,15: 1 327–1 337.

[11] DO Y J, YOUNG H K. Development of ultracapacitor modules for 42-V automaotive electrical system[J]. *Journal of Power Sources,* 2003, 114: 366–373.

[12] MAJOR J. Hybrid shuttle bus using ultracapacitors[J]. *IEEE*, 2005: 275–278.

[13] WEI Tongzhen, WANG Sibo. Performance analysis and comparision of ultracapacitor based regenerative braking system[C]//*Proceeding of 2009 IEEE International Conference on Applied Superconductivity and Electromagnetic Devices,*Chengdu, China, September 25-27, 2009: 3 405–3 410.

[14] XU Aiguo, XIE Shaojun. Dynamic voltage equalization for series-connected ultracapacitors in EV/HEV applications[J]. IEEE Transactions on Vehicular Technology, 2009, 58(8): 3 981–3 987.

[15] CAO Jian, EMADI A. A new battery / ultra - capacitor hybrid energy storage system for electric, hybrid and plug-in hybrid electric vehicles[J]. *IEEE,* 2009: 941–945.

[16] YAN Xinxiang, PATTERSON D. Novel power management for high performance and cost reduction in an electric vehicle[J]. *Renewable Energy*, 2001, 22: 177–183.

[17] AHMED S, CHMIELEWSKI D J. Load characteristics and control of a hybrid fuel cell / battery vehicle[C]// *2009 American control conference,* Hyatt Regency Riverfront, St. Louis, MO, USA, June 10–12, 2009: 2 654–2 659.

[18] LU Shuai, CORZINE K. Unique ultracapacitor direct integration schemein multilevel motor drives for large vehicle propulsion[J]. *IEEE transactions on vehicular vehicular technology*, July 2007, 56(4): 1 506–1 515.

[19] DIXON J W, ORTUZAR M E. Ultracapacitor +DC-DC converters in regenerative braking system[J]. *IEEE AESS Systems Magazine*, 2002: 16–21.

[20] MOHAMED Y A R I. Design and implementation of a robust current-control scheme for a PMSM vector drive with a simple adaptive disturbance observer[J]. *IEEE transactions on industrial electronics,* August 2007, 54(4): 1 981–1 988.

[21] LIN Hai, LI Hong. On inverter fault-tolerant operation vector control of a PMSM drive[J]. *IEEE,* 2009: 522−526.

## Biographical notes

BIAN Yongming, born in 1966, is currently a professor and a PhD candidate supervisor at *School of Mechanical Engineering, Tongji University, China*. His main reserch interest is real-time network for complex heavy mechanical system.
E-mail：ymbianmail@163.com

ZHU Lijing, born in 1980, is currently a PhD candidate at *School of Mechanical Engineering, Tongji University, China*. Her research interest is the key technology of hybrid electrical driven for construction machinery and equipment.
Tel: +86-13621712105; E-mail: zhulijing126@126.com

LAN Hao, born in 1986, is currently a master candidate at *School of Mechanical Engineering, Tongji University, China*. His main reserch interest is electrical control technology and network control theory.
E-mail：332931704@qq.com

LI Anhu, born in 1975, is a PhD candidate supervisor at *School of Mechanical Engineering, Tongji University, China*. His main reserch interests include dynamic testing and remote monitoring of engineering machinery.
E-mail：yfliah@yahoo.com.cn

XU Xinming, born in 1982, is currently a PhD candidate at *School of Mechanical Engineering, Tongji University, China*. His main reserch interest is Electrical control technology and network control theory.
E-mail：fengping14@163.com